ЖЭТФ, 2015, том 148, вып. 6 (12), стр. 1155–1168

PBE–DFT THEORETICAL STUDY OF ORGANIC PHOTOVOLTAIC MATERIALS BASED ON THIOPHENE WITH 1D AND 2D PERIODIC BOUNDARY CONDITIONS

K. Saïl[a*], **G. Bassou**[a], **M. H. Gafour**[b], **F. Miloua**[a]

[a] *Laboratoire de Microscopie, Microanalyse de la Matière et Spectroscopie Moléculaire (L2MSM),*
Faculté des Sciences Exactes, Université Djillali Liabès
22000, Sidi Bel Abbès, Algérie

[b] *Centre Universitaire Ahmed Zabana de Rélizane,*
Institut des Sciences Exactes et Sciences de la Nature et de la Vie, Département de Chimie
48000, Rélizane, Algérie

Received May 6, 2015

Conjugated organic systems such as thiophene are interesting topics in the field of organic solar cells. We theoretically investigate π-conjugated polymers constituted by n units ($n = 1$–11) based on the thiophene (Tn) molecule. The computations of the geometries and electronic structures of these compounds are performed using the density functional theory (DFT) at the 6–31 G(d, p) level of theory and the Perdew–Burke–Eenzerhof (PBE) formulation of the generalized gradient approximation with periodic boundary conditions (PBCs) in one (1D) and two (2D) dimensions. Moreover, the electronic properties (HOCO, LUCO, E_{gap}, V_{oc}, and V_{bi}) are determined from 1D and 2D PBC to understand the effect of the number of rings in polythiophene. The absorption properties — excitation energies (E_{ex}), the maximal absorption wavelength (λ_{max}), oscillator strengths, and light harvesting efficiency are studied using the time-dependent DFT method. Our studies show that changing the number of thiophene units can effectively modulate the electronic and optical properties. On the other hand, our work demonstrates the efficiency of theoretical calculation in the PBCs.

DOI: 10.7868/S0044451015120111

1. INTRODUCTION

In recent years, organic solar cells of conjugated polymers such as those based on thiophene have shown improved efficiencies. Consequently, organic photovoltaic (OPV) cells that offer the advantages of a relatively low fabrication cost compared to silicon-based materials, easy processing, flexibility, and possible recyclability, have gained focus despite their relatively low efficiencies [1]. Indeed, there are other important factors affecting the device overall efficiency and performance, i. e., the charge carrier mobility, the charge extraction at the electrodes [2], and photochemical stability. On the other hand, the development of organic solar cells has progressed rapidly with the synthesis of new organic materials, control of the processing condition such as annealing, and the use of additive [3] as well as the introduction of various device structures such as the tandem and inverted structures [4–6]. The significant improvement of OPV device performance has been accomplished by introducing various OPV architectures, such as bulk-heterojunction (BHJ) and inverted device structures, and developing low-band-gap conjugated polymers and innovative organic small molecules as donor materials. However, a new type of solar cells has attracted considerable attention due to their environmental friendliness and low cost of production. Therefore, further study is required to increase the efficiency, improve the lifetime, and reduce the production costs before the low-cost goal can be achieved. Up to now, main efforts have focused on improving the photovoltaic conversion efficiency, and recently about 8 % of white light efficiency has been realized on the device level. It is generally considered that a minimum power conversion efficiency of 10 % is needed in order to enable realistic applications, in building integrated OPV cells.

---

[*] E-mail: sailkari7@yahoo.com

The major differences between the underlying physics of organic solar cells and their inorganic relatives come from the low mobility (between 1 and 10^{-5} cm^2/V·s) of the charge carriers as well as the low dielectric constant, which results in strong Coulomb interaction between electrons and holes after photoexcitation [7].

The appropriate highest occupied molecular orbital (HOMO), lowest unoccupied molecular orbital (LUMO) energy level of the donors and acceptors, and a low band gap are known to be important for high OPV performance, as well as good film-forming properties, strong absorption ability, and high charge mobility [8]. Their performance is known to be limited by the small charge-generating interfacial area between the donor and acceptor layers [9]. Significant efforts have been devoted to developing methods for controlling the band gaps and the positions of the HOMO and LUMO of conjugated materials with the goal to produce technologically useful low-band-gap polymers.

Theoretical analysis of the electronic structure of conjugated systems can establish the relation between molecular structure and electronic properties [10]. The values of HOCO (highest occupied crystal orbital)/LUCO (lowest unoccupied crystal orbital) and gap energies can be estimated by density functional theory calculations [11–14] with different basis sets. Therefore, the DFT theoretical calculations give a good description of the absorption properties of the studied compound and can be used to predict the electronic characteristics of other materials.

Up to now, the photoactive materials for organic solar cells have been the subject of several theoretical studies [15–28]. However, it is important to understand the nature of the relation between the molecular structure and the electronic properties to provide guidelines for the development of new materials and the necessity to benefit from their adaptive properties to photovoltaic cells.

Different compounds with conjugated backbones can be used as the electron donor material in OPV devices. In particular, polythiophene and its related compounds have attracted considerable attention over the past decade in view of their potential applications to electronic and optoelectronic devices. The choice of this compound depends on several parameters including the energy gap.

The use of low-band-gap materials is a viable method for better harvesting the solar spectrum and increasing its efficiency [29]. The control of this parameter of the materials is a research issue of ongoing interest. In this paper, quantum chemical investigation is performed to explore the geometric, electronic, and optical properties of these compounds with the aim to evidence the relation between molecular structure and optoelectronic properties.

2. METHODOLOGY AND COMPUTATIONAL DETAILS

In the present study, DFT calculations are carried out for thiophene-derived conjugated polymers $(C_4H_4S)_n$, where n denotes the number of thiophene units ($n = 1$ to 11). We first performed B3LYP/6-31G (d,p) calculations in order to obtain the optimized conformations. This choice was made according to [30]; the B3LYP calculations give reasonable structures. The calculations were carried out using the GAUSSIAN 09-D package [31]. The visualization of any molecule was carried out using GaussView 05 program [32].

All molecular calculations of optimized structures were performed in the gas phase using the DFT [33, 34] combined with the 6-31G (d,p) level of theory. For the periodic boundary conditions (PBCs) in one and two dimensions, the Perdew–Burke–Eenzerhof (PBEPBE) [35–37] formulation of the generalized gradient approximation to the exchange correlation functional was used. The HOCO, LUCO, and energy gap of the studied compounds have been calculated and are reported.

To gain insight into the optical properties, the excitation energy and UV/Vis absorption spectra for the singlet–singlet transition of all compounds were simulated using the time-dependent DFT with a B3LYP functional combined with the 6-31G (d,p) level of theory. Applications of the time-dependent DFT have become reliable approaches for the theoretical treatment of electronic excitation processes, and recent works demonstrate the good accuracy for a wide range of organic systems [38–40]. The maximum open circuit voltage (V_{oc}) of an organic solar cell is related to the difference between the HOMO of the electron donor and the LUMO of the electron acceptor. The values of V_{oc} can be calculated from the empirical formula [41]

$$V_{oc} = |E_{HOMO}(\text{Donor})| - \\ - |E_{LUMO}(\text{Acceptor})| - 0.3. \quad (1)$$

The light harvesting efficiency (LHE) of the compounds has to be as high as possible to maximize the photocurrent response. Here, LHE is expressed as [42]

$$\text{LHE} = 1 - 10^{-f}, \quad (2)$$

where f is the absorption (oscillator strength) of the compound associated with λ_{max}. The oscillator

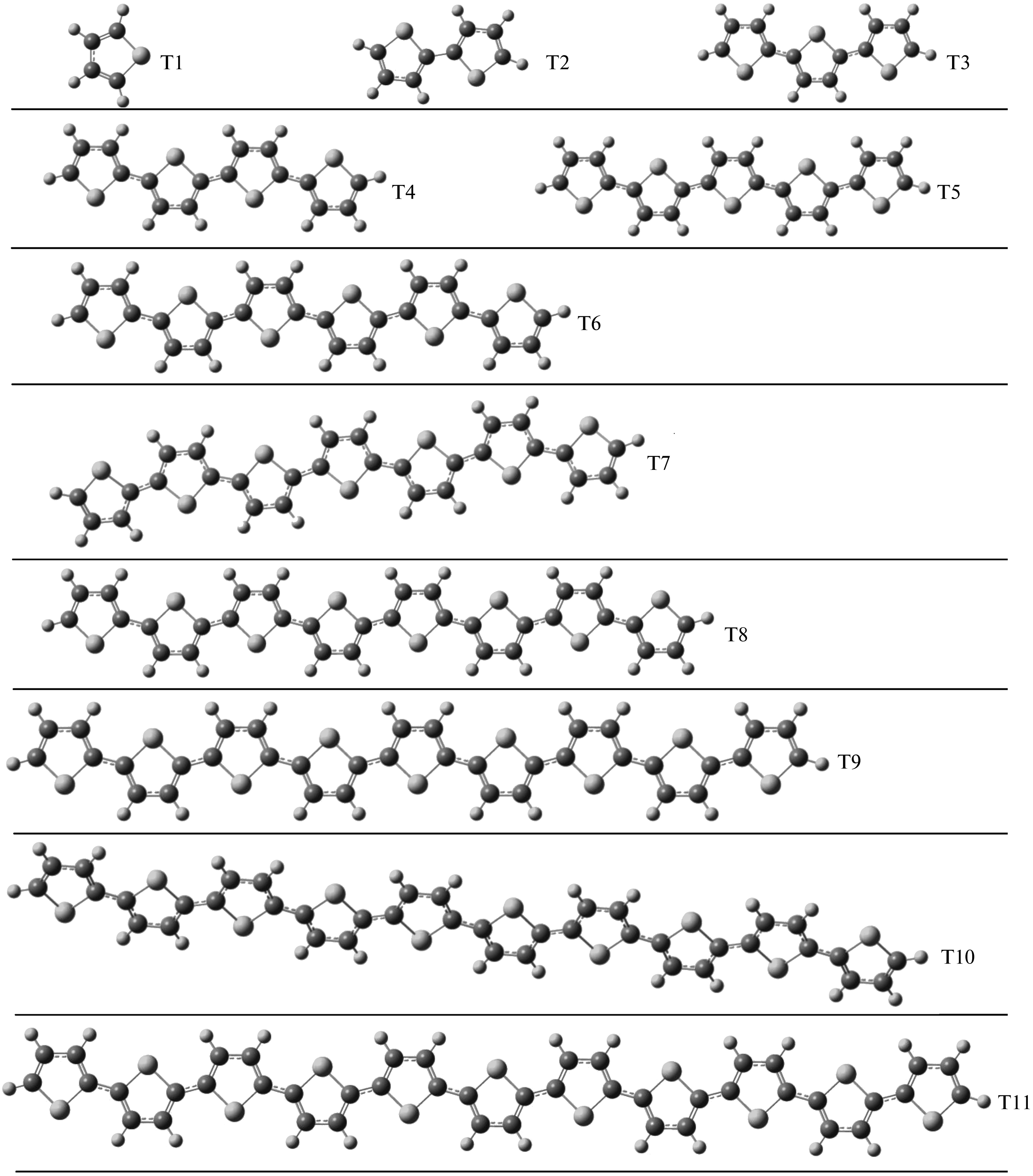

Fig. 1. Optimized structure of the studied compounds by the B3LYP/6-31G(d,p) level

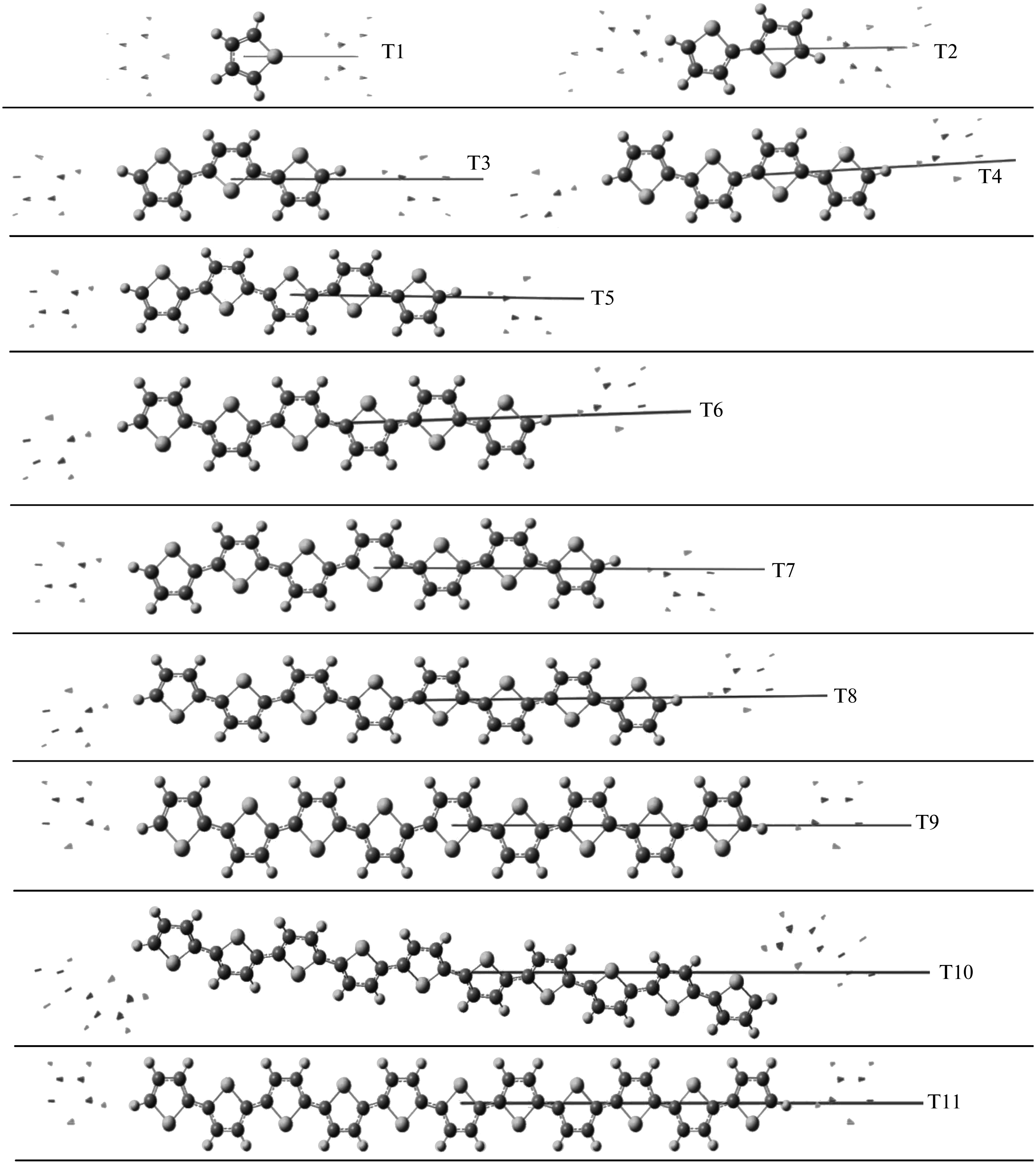

Fig. 2. Optimized structure of the studied compounds by the PBEPBE/6-31G(d, p) level using 1D PBC

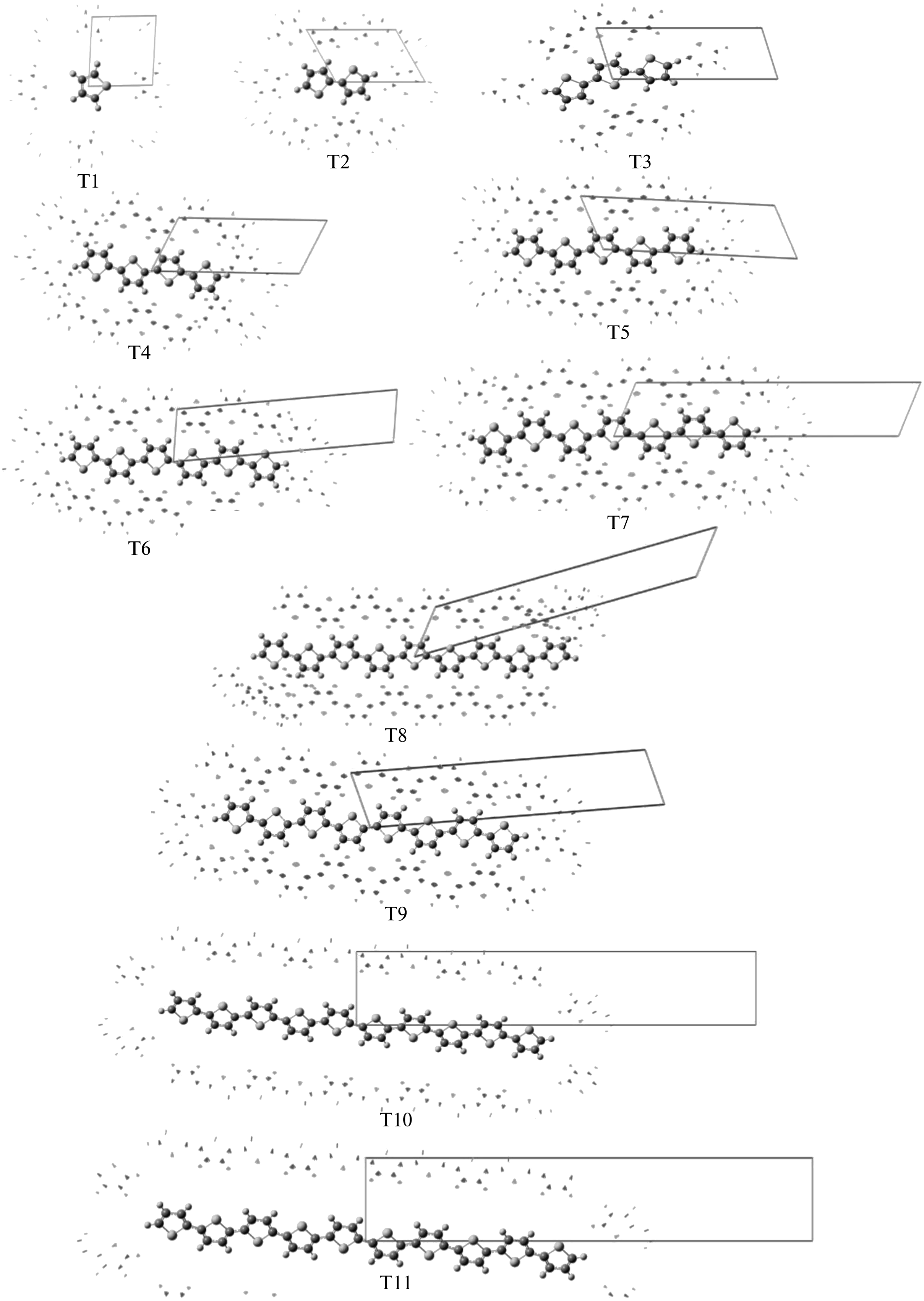

Fig. 3. Optimized structure of the studied compounds by the PBEPBE/6-31G(d,p) level using 2D PBCs

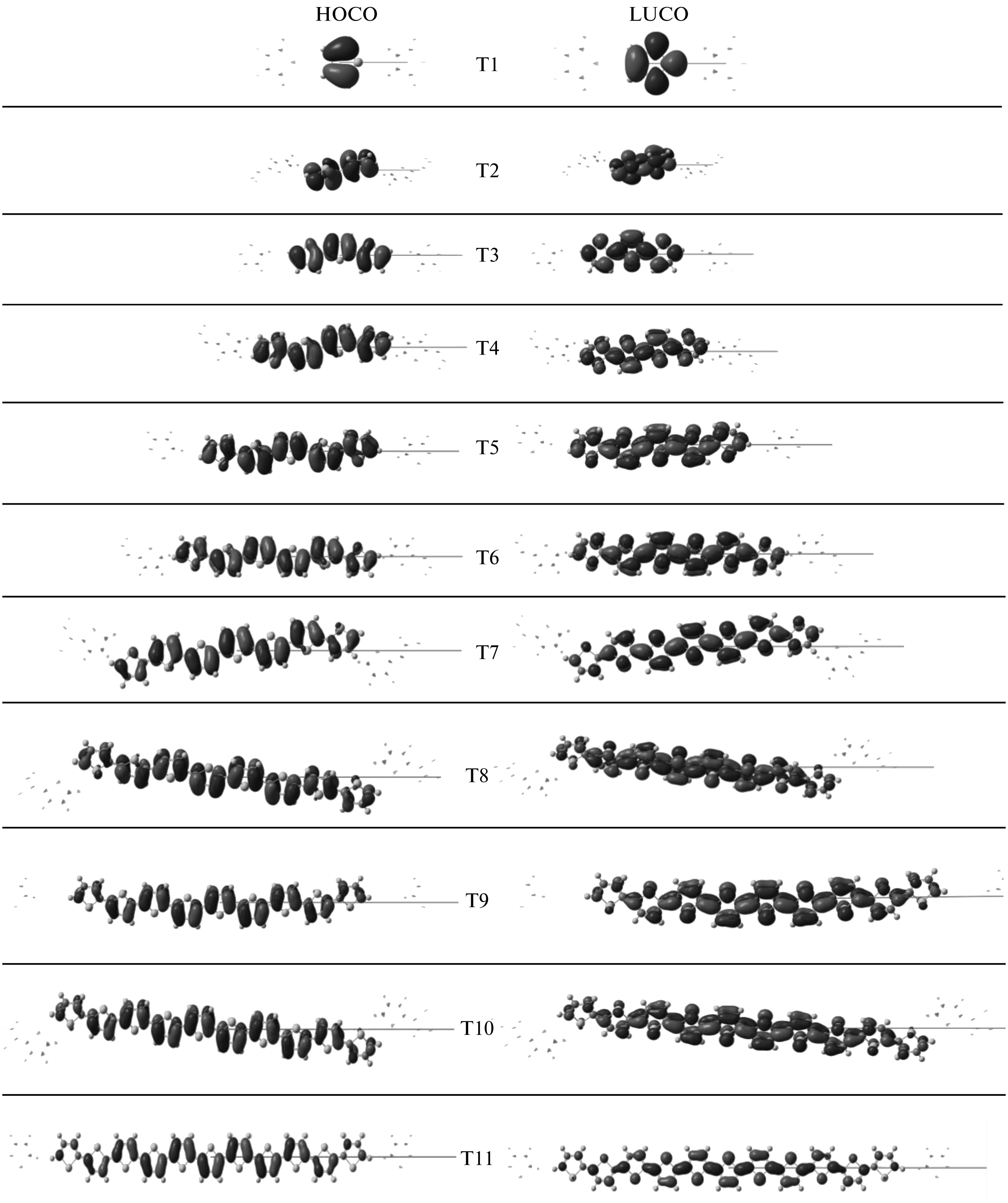

Fig. 4. The contour plot of HOCO and LUCO orbitals of the studied compounds using 1D PBC

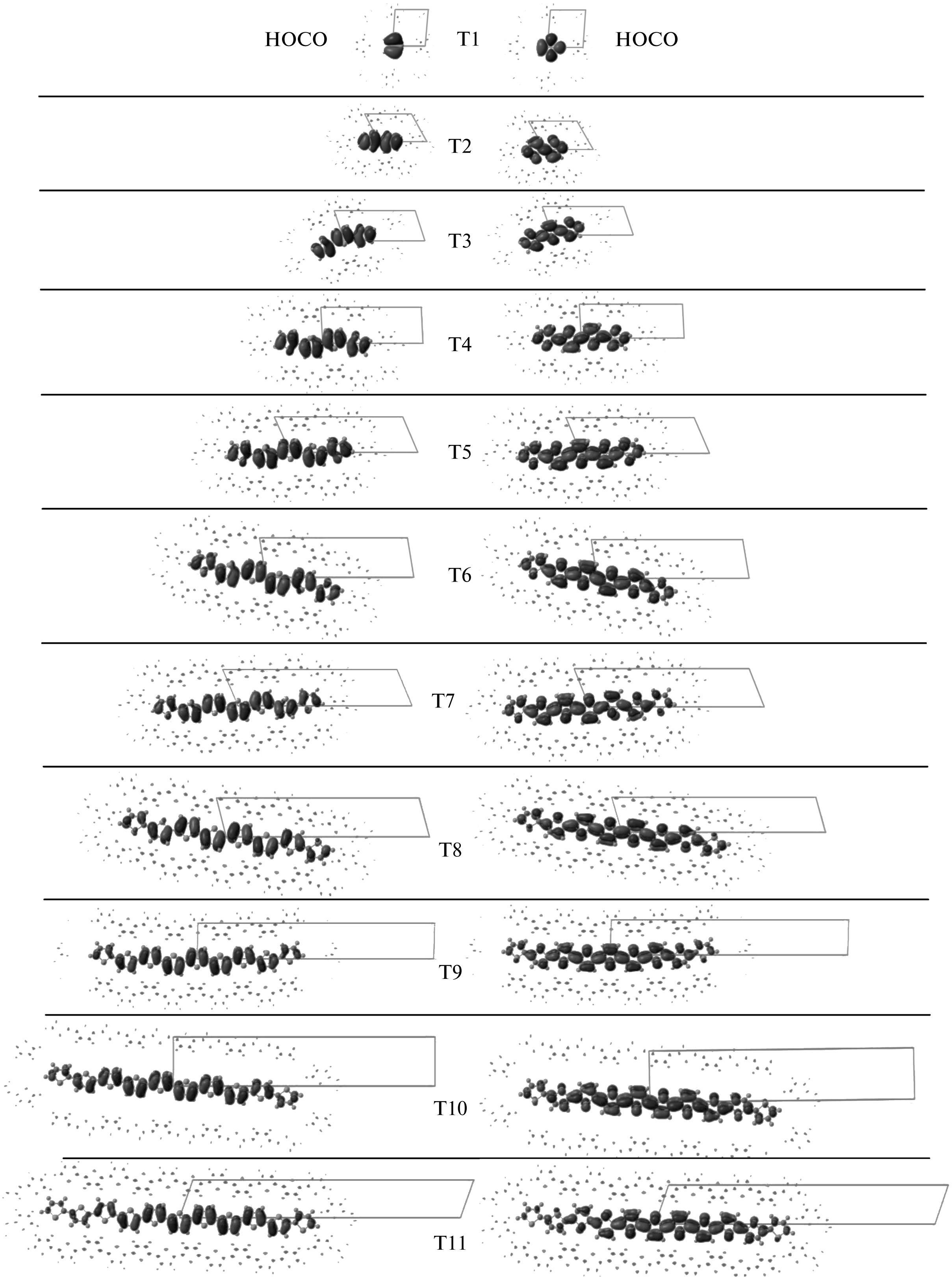

Fig. 5. The contour plot of HOCO and LUCO orbitals of the studied compounds using 2D PBCs

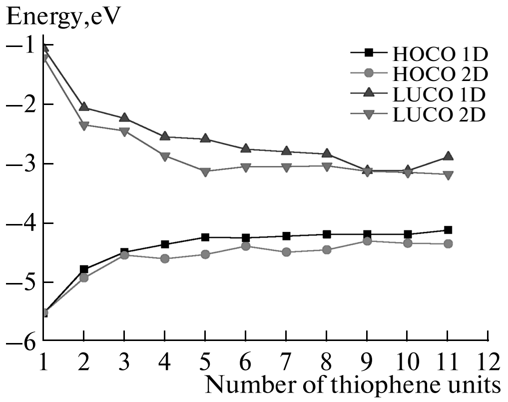

Fig. 6. HOCO and LUCO of the studied compounds plotted as functions of the number of thiophene rings calculated at the PBEPBE/6-31G(d,p) using 1D PBCs and 2D PBCs

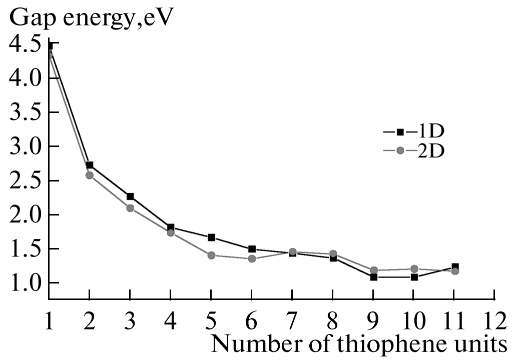

Fig. 7. Energy gap of the studied compounds plotted as a function of the number of thiophene rings calculated at the PBEPBE/6-31G(d,p) using 1D PBCs and 2D PBCs

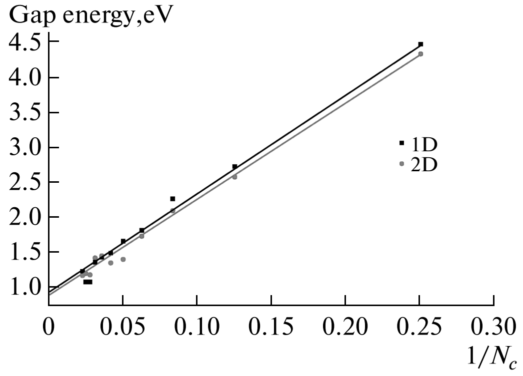

Fig. 8. Energy gap of the studied compounds plotted as a function of the inverse number N_c of the carbon atoms along the conjugated chain calculated at the PBEPBE/6-31G(d,p) using 1D PBCs and 2D PBCs

strength is directly derived from the time-dependent DFT calculations.

3. RESULTS AND DISCUSSION

The optimized structures of all studied compounds are illustrated in Fig. 1. All the molecular geometries have been calculated with the hybrid B3LYP function combined with 6-31G(d,p) basis sets. The obtained structures are optimized again in PBCs using the PBEPBE/6-31G(d,p) level of theory. The optimized geometries obtained for the compounds in one dimension (1D) and two dimensions (2D) are shown in Figs. 2 and 3. We can clearly see the π-electron delocalization between the different aromatic units. On the other hand, results of the optimized structures for all studied compounds show that the planar structure is mostly stable in all oligo- and polythiophenes.

It is very important to analyze the HOCO and the LOCO for these compounds, because the latter provides a rational qualitative indication of the excitation properties and of the ability of electron or hole transport. On the other hand, the HOCO and the LUCO energy levels of the donor and acceptor components are very important factors to determine whether effective charge transfer occurs between the donor and the acceptor. The isodensity plots of the model compounds are shown in Figs. 4 and 5 and calculated frontier orbital energy and energy gaps for all considered molecules are given in Table 1.

Figures 4 and 5 show that the HOCO and LUCO of all molecules are spread over the whole p-conjugated backbones with similar character; the HOCOs display the antibonding character between two adjacent fragments and the bonding character within each unit. But the LUCOs exhibit the bonding character between two adjacent fragments. We note that the heteroatoms have no HOCO lobes, as has been reported earlier [43]. From Figs. 4 and 5, it is clear that the HOCOs are principally composed of ring C=C bonds and the LUMOs are principally composed of inter-ring formal C–C single bonds. The same results were obtained in [44].

The calculated HOCOs energies are in the range −5.54 eV to −4.14 eV for 1D PBCs and −5.53 to −4.34 for 2D PBCs. However, the HOCO energies were in the respective range −2.91 to −1.08 and −3.20 to −1.24 for 1D PBCs and 2D PBCs. According to the graph shown in Fig. 6, the HOCO energy decreases sharply for the compounds with $n = 1$ to those with $n = 4$ (where n is

Table 1. The HOCO energy, the LUCO energy, the gap energy, the open-circuit voltage V_{oc}, and the built-in potential V_{bi} of studied compounds obtained by the PBEPBE/6-31G(d,p) level using 1D and 2D PBCs. n is the number of thiophene units

Compound	n	HOCO, eV		LUCO, eV		Gap, eV		V_{oc}/C_{60}, eV		V_{bi}, eV	
		1D	2D	1D	2D	1D	2D	1D	2D	1D	2D
T1	1	−5.54	−5.53	−1.08	−1.24	4.45	4.31	0.26	0.27	2.07	2.06
T2	2	−4.80	−4.94	−2.08	−2.37	2.71	2.56	1	0.86	1.33	1.47
T3	3	−4.51	−4.56	−2.26	−2.47	2.25	2.08	1.29	1.24	1.04	1.09
T4	4	−4.38	−4.62	−2.57	−2.89	1.80	1.72	1.42	1.18	0.91	1.15
T5	5	−4.26	−4.55	−2.61	−3.15	1.65	1.39	1.54	1.25	0.79	1.08
T6	6	−4.27	−4.41	−2.78	−3.07	1.48	1.34	1.53	1.39	0.8	0.94
T7	7	−4.24	−4.51	−2.82	−3.07	1.42	1.44	1.56	1.29	0.77	1.04
T8	8	−4.21	−4.47	−2.86	−3.06	1.35	1.41	1.59	1.33	0.74	1
T9	9	−4.21	−4.32	−3.14	−3.15	1.07	1.17	1.59	1.48	0.74	0.85
T10	10	−4.21	−4.36	−3.14	−3.17	1.07	1.19	1.59	1.44	0.74	0.89
T11	11	−4.14	−4.37	−2.91	−3.20	1.22	1.16	1.66	1.43	0.67	0.9

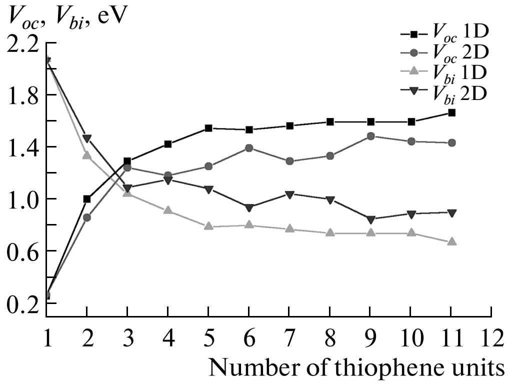

Fig. 9. Open circuit voltage V_{oc} and the built-in potential V_{bi} of the studied compounds plotted as functions of the number of thiophene rings calculated using Eq. (1)

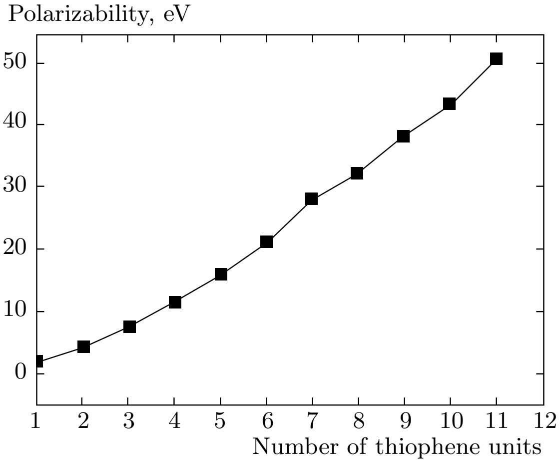

Fig. 10. Polarizability of the studied compounds plotted as a function of the number of thiophene rings calculated using the time-dependent DFT

number of rings) and slightly for the compounds with $n > 4$. The LUCO energy decreases strongly in the range 1 to 4 and slightly for $n > 4$.

In material science, band structure has become important because the band gap is one of the most important factors for controlling the physical properties of solar cells. The band gaps in conjugated polymers are governed by their chemical structures. Their value can be defined by the difference between the lowest band energy in the conduction band and the highest band energy in the valence band.

For 1D PBCs, the calculated band gap of the studied compounds decreases gradually with increasing the number of rings from $n = 1$ to $n = 10$. In [45], it was also noted that the energy gap decreases as the chain is elongated. The same observation was noted for 2D PBC calculated band gap with the number of rings from $n = 1$ to $n = 6$. When the backbone of a conjugated polymer is twisted, the π orbital overlap decreases, resulting in a decrease in the effective conjugation length, which is the case of compounds in the

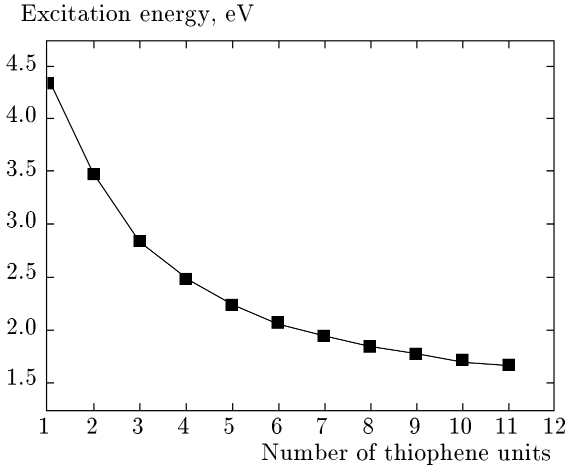

Fig. 11. Excitation energy of the studied compounds plotted as a function of the number of thiophene rings calculated using the time-dependent DFT

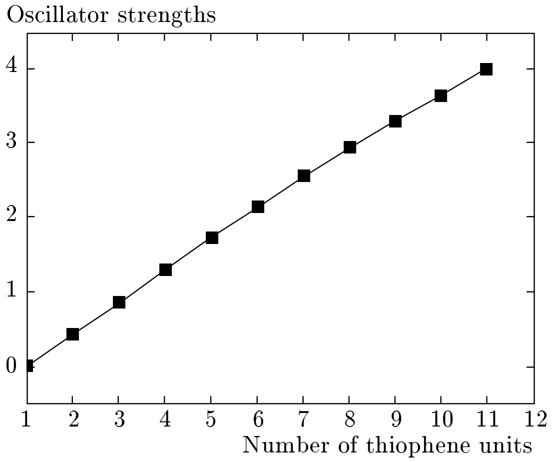

Fig. 12. Oscillator strengths of the studied compounds plotted as a function of the number of thiophene rings calculated using the time-dependent DFT

range from $n = 7$ to $n = 11$. On the other hand, interchain interactions also have a strong effect on the electronic properties of conjugated polymers. Furthermore, strong π-stacking interactions lead to significant shifts of the band gap. The size and direction of the shift also depend strongly on the relative orientation of neighboring chains [46, 47].

The calculated band gaps are in the respective range 1.07–2.71 eV and 1.16–2.56 eV for 1D PBCs and 2D PBCs with the number of rings $n > 1$. The experimental in [48] give a value in the range 2.0–2.2 eV. Low-band-gap polymers ($E_g < 2.0$ eV) are desired for solar cell application [49] because the polymer can absorb more solar energy.

The highest values are those obtained for the monothiophene, 4.45 eV for 1D PBCs and 4.31 eV for 2D PBCs (Fig. 7). These values are reduced by 1.74 eV for bithiophene and 2.2 eV for trithiophene. The calculated values of mono-, bi-, and trithiophene are approximately similar to those obtained in [50] (4.49 eV, 2.93 eV, and 2.21 eV respectively).

Theoretical studies of polymers generally extrapolate oligomer properties to infinite chain lengths [51, 52]. In general, such an approach should be similar to using the periodic boundary calculation approximation. The band gap for infinite chains of polymers can be determined by plotting band gaps in polymers against the inverse number N_c of the carbon atoms along the conjugated chain and extrapolating this number to infinity according to the linear equation [12]

$$E_g(N_c) \approx \frac{a}{N_c} + b \tag{3}$$

with b determined by linear regression.

According to the graph shown in Fig. 8, the band gap is extrapolated to be 0.93 eV for 1D PBCs and 0.88 eV for 2D PBCs.

The maximum open-circuit voltage (V_{oc}) of a solar cell is related to the difference between the HOMO of the donor (our studied molecules) and the LUMO of the electron acceptor [53] (PCBM(C60) derivatives in our case). Figure 9 shows that V_{oc} increases with increasing the number of rings, inversely to the variation of α, which decreases with increasing the number of rings.

The open-circuit voltage V_{oc} is related to the built-in potential denoted by V_{bi}, which is primarily determined by the relative energy gap between the HOMO of the donor and the LUMO of the acceptor [54]. The built-in potential V_{bi} across a solar cell is usually described as an upper limit of the open-circuit voltage of the cell under illumination. Their values are between 0.67 and 2.07 for 1D PBCs and between 0.85 and 2.06 for 2D PBCs.

Due to the high symmetry of the compounds corresponding to an even number of rings, the values of the electric dipole moment are very small. For an odd number of rings, the values are close to 0.62 D. Generally, orientations of the polymer chains are the most important parameters affecting the electric charge transport properties of polymers; the electrical conductivity of a polymer chain is altered when its orientation and consequently its symmetry and nonisotropic interactions are changed [55].

Values of polarizabilities and hyperpolarizabilities

Table 2. Dipole moment μ, polarizability α, hyperpolarizability β, excitation energy E_{ex}, oscillator strengths f, wavelength λ_{max}, and LHE of the studied compounds obtained by the time-dependent DFT using 1D and 2D PBCs. n is the number of thiophene units

Compound	n	μ, D	α, eV	β, arb. units	E_{ex}, eV	f	λ, nm	LHE
T1	1	0.62	1.85	21.08	4.35	0	284.83	0
T2	2	0.0004	4.26	0.0028	3.47	0.43	357.00	0.63
T3	3	0.63	7.47	501.38	2.85	0.84	434.36	0.85
T4	4	0.0003	11.45	0.00002	2.49	1.28	497.39	0.94
T5	5	0.63	16.05	1055.74	2.25	1.72	550.84	0.98
T6	6	0.0006	21.14	0.74	2.08	2.14	596.67	0.99
T7	7	0.58	28.25	2199.94	1.95	2.54	635.83	0.99
T8	8	0.0002	32.33	0.27	1.85	2.93	669.04	0.99
T9	9	0.63	38.25	1193.88	1.78	3.30	696.87	0.99
T10	10	0.001	43.24	0.030	1.72	3.65	720.02	0.99
T11	11	0.63	50.50	1172.24	1.67	3.99	739.58	0.99

for all compounds have been calculated and listed in Table 2. Based on Fig. 10, we can claim that with an increase of the number of rings, polarization values increase as well. An increase in the chain length of a conjugated polymer (or the length of the π-conjugated system) increases the polarizability values of the polymer. It was shown in [56] that the bond length alternation as a parameter related to the molecular structure strongly affects the values of the linear polarizability and hyperpolarizability of organic compounds with delocalized π-electron systems.

The excitation to the S_1 state corresponds almost exclusively to the promotion of an electron from the HOMO to the LUMO orbital. The excitation energies represented in Fig. 11 decreases gradually as the ring number increases. In the case of the oscillator strength (Fig. 12), the absorption wavelengths arising from the $S_0 \to S_1$ electronic transition increase progressively with an increase in conjugation lengths. It is to be affected by the electron-donating capability from π-conjugation and heteroaromatic groups [57].

The theoretical absorption spectra presented in Fig. 13 are calculated by using the time-dependent DFT approach. The maximum absorptions in UV/Vis spectra are dominated by HOMO→LUMO $\pi \to \pi^*$ transitions. Furthermore, the absorption properties are an important factor for applications as a photovoltaic material, and a good photovoltaic material should have broad and strong visible absorption characteristics. The calculated wavelength λ_{max} of the studied compounds increases with increasing the conjugation length (Fig. 14). This bathochromic effect is obviously due to a higher mean conjugation length and to the interchain electronic coupling [58].

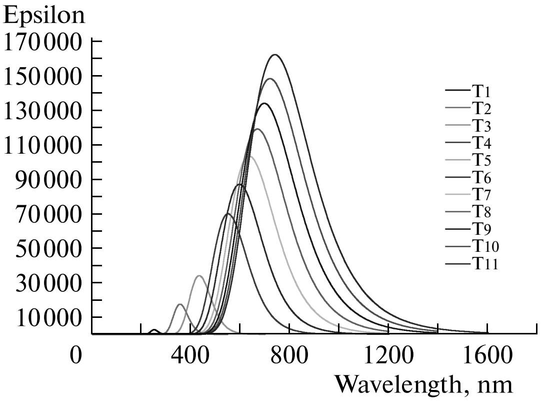

Fig. 13. UV/V is spectra of the studied compounds plotted as functions of the number of thiophene rings calculated using the time-dependent DFT

LHE is a good indicator of the incident photon-to-electron conversion efficiency (IPCE). Figure 15 shows that for $n = 1$ to $n = 4$, the LHE increases slightly. However, for $n > 4$, the LHE value remains constant, being close to 0.99. Therefore, the compounds having $n > 4$ give similar photocurrent.

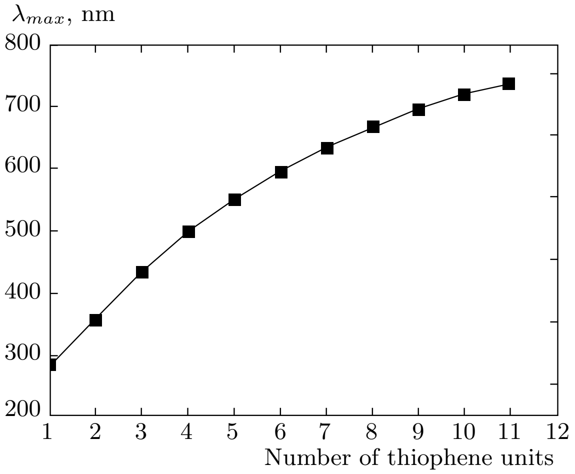

Fig. 14. Wavelength λ_{max} of the studied compounds plotted as a function of the number of thiophene rings calculated using the time-dependent DFT

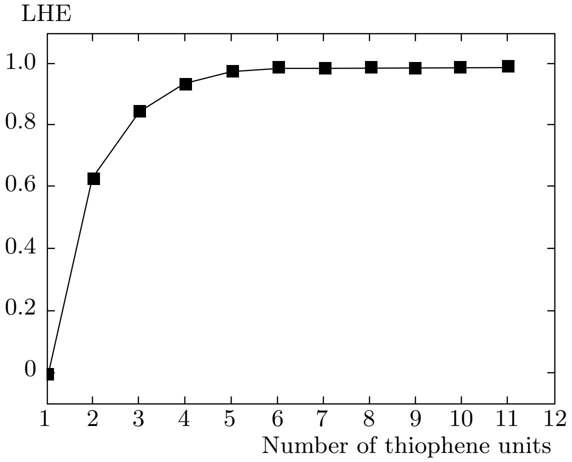

Fig. 15. LHE of the studied compounds plotted as a function of the number of thiophene rings calculated using Eq. (2)

4. CONCLUSION

This study is a theoretical analysis of the geometrical, optical, and electronic properties of various compounds based on thiophene, which displays the effect of the number of rings on the structural and optoelectronic properties of these materials. Theoretical calculations of optimized structures were performed using the density functional theory with periodic boundary conditions in one and two dimensions, where the Perdew–Burke–Eenzerhof formulation was used. The calculated values of the HOCO, the LUCO, the gap energy, and V_{oc} of the studied molecules can give an idea on the possibility of efficient electron injection. It was also found that changing the number of thiophene units can effectively modulate the electronic and photophysical properties of these compounds. On the other hand, optical properties of all compounds were simulated using the time-dependent DFT with the B3LYP functional combined with the 6-31G (d, p) level of theory. The results show that this procedure of theoretical calculations can be employed to predict the optoelectronic properties of other compounds, and further to design novel materials for organic solar cells. Furthermore, the PBC model demonstrates a powerful approach and can be used as a model system for understanding the relation between electronic properties and molecular structure.

REFERENCES

1. P. L. T. A. Boudreault, A. Najari, and M. Leclerc, Chem. Mater. **23**, 456 (2010).
2. R. Po, C. Carbonera, A. Bernardia, and N. Camaioni, Energy Environ. Sci. **4**, 285 (2011).
3. H.-C. Liao, C.-C. Ho, C.-Y. Chang, M.-H. Jao, S. B. Darling, and W.-F. Su, Mater. Today **16**, 326 (2013).
4. J. You, L. Dou, Z. Hong, G. Li, and Y. Yang, Prog. Polym. Sci. **38**, 1909 (2013).
5. L.-M. Chen, Z. Hong, G. Li, and Y. Yang, Adv. Mater. **21**, 1434 (2009).
6. C. Yi and X. Gong, Curr. Opin. Chem. Eng. **2**, 125 (2013).
7. M. Jaiswal and R. Menon, Polym. Int. **55**, 1371 (2006).
8. S. A. Jenekhe and S. Yi, Appl. Phys. Lett. **77**, 2635 (2000).
9. M. Granstrom, K. Petritsch, A. C. Arias, A. Lux, M. R. Andersson, and R. H. Friend, Nature **395**, 257 (1998).
10. J. Cornil, D. Beljonne, J.-P. Calbert, and J.-L. Brédas, Adv. Mater. **13**, 1053 (2001).
11. C. Risko, M. D. McGehee, and J. L. Bredas, Chem. Sci. **2**, 1200 (2011).
12. S. Yang, P. Olishevski, and M. Kertesz, Synth. Met. **141**, 171 (2004).
13. J. Gierschner, J. Cornil, and H. J. Egelhaaf, Adv. Mater. **19**, 173 (2007).

14. J. Casanovas and C. Alemán, J. Phys. Chem. C **111**, 4823 (2007).

15. S. C. Price, A. C. Stuart, L. Yang, H. Zhou, and W. You, J. Amer. Chem. Soc. **133**, 4625 (2011).

16. G. Dennler, M. C. Scharber, T. Ameri, P. Denk, K. Forberich, C. Waldauf, and C. J. Brabec, J. Adv. Mater. **20**, 579 (2008).

17. M. C. Scharber, D. Wuhlbacher, M. Koppe, P. Denk, C. Waldauf, A. J. Heeger, and C. L. Brabec, Adv. Mater. **18**, 789 (2006).

18. K. M. Coakley and M. D. McGehee, Chem. Mater. **16**, 4533 (2004).

19. C. P. Chen, S. H. Chan, T. C. Chao, C. Ting, and B. T. Ko, J. Amer. Chem . Soc. **130**, 12828 (2008).

20. S. H. Chan, C. P. Chen, T. C. Chao, C. Ting, C. S. Lin, and B. T. Ko, Macromolecules **41**, 5519 (2008).

21. C. Y. Yu, C. P. Chen, S. H. Chan, G. W. Hwang, and C. Ting, Chem. Mater. **21**, 3262 (2009).

22. J. P. Lu, F. S. Liang, N. Drolet, J. F. Ding, and Y. Tao, Chem. Commun. **42**, 5315 (2008).

23. J. H. Tsai, C. C. Chueh, M. H. Lai, C. F. Wang, W. C. Chen, B. T. Ko, and C. Ting, Macromolecules **42**, 1897 (2009).

24. M. H. Lai, C. C. Chueh, W. C. Chen, J. L. Wu, and F. C. Chen, J. Polym. Sci. Part A **47**, 973 (2008).

25. M. Westphalen, U. Kreibig, J. Rostalski, H. Lüth, and D. Meissner, Sol. Energy Mater. Sol. Cells **61**, 97 (2000).

26. Y. Kim, S. Cook, S. M. Tuladhar, S. A. Choulis, J. Nelson, J. R. Durrant, D. D. C. Bradley, M. Giles, I. McCulloch, C. S. Ha, and M. Ree, Nat. Mater. **5**, 197 (2006).

27. J. Peet, J. Y. Kim, N. E. Coates, W. L. Ma, D. Moses, A. J. Heeger, and G. C. Bazan, Nat. Mater. **6**, 497 (2007).

28. W. Y. Wong, X.-Z. Wang, Z. He, A. B. Djuri, C.-T. Yip, K.-T. Cheung, H. Wang, C. S. K. Mak, and W.-K. Chan, Nat. Mater. **6**, 521 (2007).

29. Y.-J. Chen, S.-H. Yang, and C.-S. Hsu, Chem. Rev. **109**, 5868 (2009).

30. J.-H. Lii, B. Ma, and N. Allinger, J. Comput. Chem. **20**, 1593 (1999).

31. M. J. Frisch, G. W. Trucks, H. B. Schlegel et al., Gaussian 09, Revision D.01, Wallingford CT, USA (2009).

32. R. Dennington, T. Keith, and J. Millam, GaussView, ver. 5 (2009).

33. P. Hohenbergand and W. Kohn, Phys. Rev. B **136**, 864 (1964).

34. W. Kohn and L. J. Sham, Phys. Rev. A **140**, 1133 (1965).

35. J. P. Perdew, K. Burke, and M. Ernzerhof, Phys. Rev. Lett. **77**, 3865 (1996).

36. J. P. Perdew, A. Ruzsinszky, G. I. Csonka, O. A. Vydrov, G. A. Scuseria, L. A. Constantin, X. Zhou, and K. Burke, Phys. Rev. Lett. **100**, 136406 (2008).

37. J. P. Perdew, A. Ruzsinszky, M. Ernzerhof, G. I. Csonka, O. A. Vydrov, G. E. Scuseria, L. A. Constantin, X. Zhou, and K. Burke, Phys. Rev. Lett. **100**, 136406 (2009).

38. A. Rosa, E. J. Baerends, S. J. A. van Gisbergen, E. van Lenthe, Y. A. Groeneveld, and J. G. Snijders, J. Amer. Chem. Soc. **121**, 10356 (1999).

39. C. Adamo and V. Barone, Theor. Chem. Acc. **105**, 169 (2000).

40. P. Boulet, H. Chermette, C. Daul, Gilardoni, F. Rogemond, J. Weber, and G. Zuber, J. Phys. Chem. A **105**, 885 (2001).

41. G. Dennler, M. C. Scharber, and C. J. Brabec, Adv. Funct. Mater. **21**, 1323 (2009).

42. H. S. Nalwa, *Handbook of Advanced Electronic and Photonic Materials and Devices*, Acad. Press, San Diego CA (2001).

43. J. L. Brédas, R. L. Elsenbaumer, R. R. Chance, and R. Silbey, J. Chem. Phys. **78**, 5656 (1983).

44. G. R. Hutchison, M. A. Ratner, and T. G. Marks, J. Amer. Chem. Soc. **127**, 16866 (2005).

45. I. H. Jenkins, U. Salzner, and P. G. Pickup, Chem. Mater. **8**, 2444 (1996).

46. J. Cornil, D. A. dos Santos, X. Crispin, R. Silbey, and J. L. Bredas, J. Amer. Chem. Soc. **120**, 1289 (1998).

47. J. Cornil, D. A. dos Santos, R. Silbey, and J. L. Brédas, Synth. Met. **101**, 492 (1999).

48. T.-C. Chung, J. H. Kaufman, A. J. Heeger, and F. Wudl, Phys. Rev. B **30**, 702 (1984).

49. W.-F. Su, *Principles of Polymer Design and Synthesis*, Vol. 82. Lect. Notes Chem. Springer-Verlag, Berlin, Heidelberg (2013).

50. S. P. Rittmeyer and A. Groß, Beilstein J. Nanotechnol. **3**, 909 (2012).

51. J. Casanovas and C. Aleman, J. Phys. Chem. C **111**, 4823 (2007).

52. M. Kertesz, C. H. Choi, and S. J. Yang, Chem. Rev. **105**, 3448 (2005).

53. A. Gadisa, M. Svensson, M. R. Andersson, and O. Inganas, Appl. Phys. Lett. **84**, 1609 (2004).

54. G. Yu, J. Gao, J. C. Hummelen, F. Wudl, and A. J. Heeger, Polymer Photovoltaic Cells: Enhanced Efficiencies via a Network of Internal Donor-Acceptor Heterojunctions, Science **270**, 1789 (1995).

55. H. S. I. Beigi, Canad. J. Chem. **90**, 902 (2012).

56. W. Bartkowiak, R. Zalesny, and J. Leszczynski, Chem. Phys. **287**, 103 (2003).

57. N. Santhanamoorthi, C.-M. Lo, and J.-C. Jiang, J. Phys. Chem. Lett. **4**, 524 (2013).

58. C. Jia, J. Zhang, J. Bai, L. Zhang, Z. Wan, and X. Yao, Dyes and Pigments **94**, 403 (2012).